ton-affinity data and from a Morokuma analysis of the important electrostatic and charge-transfer terms of these protonation energies in model calculations for constrained ammonia and phosphine, we note that increased s character in the lone pairs causes a decrease in the proton affinities. Increased s character decreases the lone-pair density in the region of the added proton, making the electrostatic energy term less favorable. The less favorable overlap between the lone-pair s character also makes the electrostatic energy less favorable. In the case of phosphirane, an additional internal bond angle strain (I-strain) increase in the conjugate acid causes the proton affinity to be unusually low.

Acknowledgments. We thank the National Science Foundation for support of this work.

Analysis of the Rotational Strength by Means of Configuration Analysis Based on the Localized Molecular Orbitals

Kazuo Akagi, Tokio Yamabe, Hiroshi Kato, Akira Imamura, and Kenichi Fukui*

Contribution from the Department of Hydrocarbon Chemistry, Faculty of Engineering, Kyoto University, Kyoto, Japan, the College of General Education, Nagoya University, Chikusa-ku, Nagoya, Japan, and the Shiga University of Medical Science, Seta, Ohtu, Japan.
Received January 21, 1980

Abstract: The n–π^* and π–π^* rotational strengths of the optically active L-5-methylpyrrolid-2-one molecule have been analyzed in detail by means of configuration analysis based on the LMO's presented here. This procedure has enabled us to evaluate simultaneously the contributions of the chromophore, substituent, and the rest of the molecule to the rotational strength of interest. The origin and effective path generating the rotational strength and their mechanisms have also been elucidated from the aspect of the intramolecular interactions between three or four molecular fragments in terms of the electronic configurations such as local and charge-transfer excitations.

I. Introduction

The rotational strengths in circular dichroism (CD) or optical rotatory dispersion (ORD) spectra have played central roles in the studies of optical activity, because of their outstanding sensitivities to the conformations and evironments.[1] The difficulties and/or ambiguities encountered in the interpretation of the rotational strengths, which have arisen from the structural complexies of molecules, have often let the investigators employ cyclic molecular systems having the restricted conformational freedom.[2] Especially, small cyclic molecules containing the peptide (amide)[3-6] and carbonyl chromophores[7] have become the focus of attention owing to their great importance in biochemistry as well as in organic chemistry. The considerable efforts to correlate the rotational strengths with the molecular structures have provided the empirical symmetry rules such as octant, quadrant, and sector rules, which are useful for defining the specific stereochemical features.[1,8,9] The approaches based on these symmetry rules, where the rotational strengths are interpreted with respect to the interaction between the chromophore and extrachromophoric moieties of a molecule, have presented the important concept of the intramolecular interaction in the chiroptical molecules,[10] by which the theoretical perturbation methods discussed later have been facilitated and developed. However, such approaches have been found to be insufficient for the explicit factorizations of the rotational strengths in terms of molecular fragments and also for the quantitative discussion, since the symmetry rules mentioned above not only permit considerable exceptions in determing the signs of the rotational strengths but also provide no features of electronic structure for interpreting the rotational strengths associated with the electronic transitions.[11]

In fact, there remain urgent problems to be solved concerning optical activity at the present stage, one of which is to clarify the origin of the optical activity determining the signs and magnitudes of the rotational strengths (e.g., inherent ring chirality and/or substituent asymmetrically linked with the chiral center).[3,5,12-14] Another is the verification of the mechanism and favorable path through which the electronic transitions of the locally symmetric chromophores are affected by the dissymmetric environment to yield the rotational strengths.[10] It is clear that these problems, that are also the subjects of our interest, are closely related to the intramolecular interaction. It follows therefore that the settlement of these problems depends upon the detailed analysis of the rotational strengths in terms of the intramolecular interaction derived from reliable theoretical calculations.

In the theoretical calculations of the rotational strengths, there have been two approaches such as perturbation methods[15-20] and

* To whom correspondence should be addressed at Kyoto University.

(1) (a) C. Djerassi, "Optical Rotatory Dispersion", McGraw-Hill, New York, 1960; (b) G. Snatzke, "Optical Rotatory Dispersion and Circular Dichroism in Organic Chemistry", Heyden, London, 1967.
(2) For instance, J. A. Schellman and E. B. Nielsen, "Conformation of Biopolymers", G. N. Ramachdran, Ed., Academic Press, New York, 1967.
(3) D. W. Urry, *Ann. Rev. Phys. Chem.*, **19**, 477 (1968).
(4) N. J. Greenfield and G. D. Fasman, *J. Am. Chem. Soc.*, **92**, 177 (1970).
(5) J. A. Schellman and S. Lifson, *Biopolymers*, **12**, 315 (1973).
(6) O. Červinka, L. Hub, F. Snatzke, and G. Snatzke, *Collect. Czech. Chem. Commun.*, **38**, 897 (1973).
(7) (a) J. P. Jennings, W. Klyne, and P. M. Scope, *J. Chem. Soc.*, 7211, 7299 (1965); (b) J. Listowski, G. Avigad, and S. England, *J. Org. Chem.*, **35**, 1080 (1970); (c) M. Keller and G. Snatzke, *Tetrahedron*, **29**, 4013 (1973); (d) T. D. Bouman and D. A. Lighter, *J. Am. Chem. Soc.*, **98**, 3145 (1976).
(8) W. Moffit, R. B. Woodward, A. Moscowitz, W. Klyne, and C. Djerassi, *J. Am. Chem. Soc.*, **83**, 4013 (1961).
(9) (a) J. A. Schellman and P. Oriel, *J. Chem. Phys.*, **37**, 2144 (1962); (b) J. A. Schellman and E. B. Nielsen, *ibid.*, **71**, 3914 (1967).
(10) (a) D. J. Caldwell and H. Eyring, "The Theory of Optical Activity", Wiley, New York, 1971; (b) A. Imamura and K. Hirao, *Tetrahedron*, **35**, 2243 (1979), see also the references therein.
(11) (a) W. Klyne, *Tetrahedron*, **13**, 29 (1961); (b) C. Ouannes and J. Jacques, *Bull. Soc. Chim. Fr.*, 3611 (1965); (c) D. N. Kirk and W. Klyne, *J. Chem. Soc., Perkin Trans. 1*, 1076 (1974).
(12) (a) H. Wolf, *Tetrahedron Lett.*, 1075 (1965): (b) M Goodman, C. Toniolo, and J. Falcetta, *J. Am. Chem. Soc.*, **91** 1816 (1969); (c) A. F. Beecham, *Tetrahedron Lett.*, 4897 (1969); (d) T. Konno, H. Meguro, and K. Tuzimura, *Tetrahedon Lett.*, 1305, 1309 (1975).
(13) (a) F. S. Richardson, D. D. Shillady, and J. E. Bloor, *J. Phys. Chem.*, **72**, 2466 (1971); (b) F. S. Richardson and R. W. Strickland, *Tetrahedron*, **31**, 2309 (1975).
(14) F. S. Richardson, R. Strickland, and D. D. Shillady, *J. Phys. Chem.*, **77**, 248 (1973).

0002-7863/80/1502-5157$01.00/0

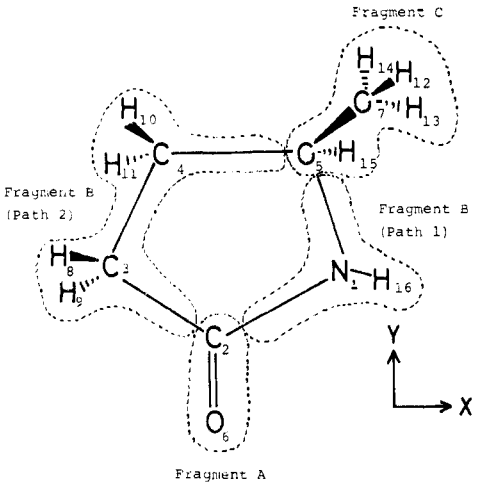

Figure 1. L-5-Methylpyrrolid-2-one.

molecular orbital (MO) methods on the basis of both semiempirical[14,21-27] and ab initio calculations.[28-31] The primary advantage of the perturbation methods is an ability to evaluate the contributions of the parts of a molecule to the rotational strengths by means of static[16] and dynamic[17] coupling treatments. Besides, these methods often make it possible to refer their results to the symmetry rules for the optical activity as mentioned above.[9,20] On the other hand, the MO's methods afford a conventional procedure owing to the direct calculation for the estimation of the rotational strength and often lead to a quantitative discussion with the aid of the configuration interaction. However, they can provide no correlation of molecular fragments effective for the analysis of the rotational strengths. This is due to the usage of delocalized (canonical) MO's generated by SCF calculations. It is therefore desired that the rotational strengths obtained by the MO methods can be interpreted in terms of molecular fragments, as in the case of the perturbation methods mentioned above.

In connection with this, one of the present authors recently developed the MO procedure by dividing the rotational strength into the contributions of two molecular subsystems[25] and furthermore proposed the method to rationalize the through-space and through-bond interactions by using localized MO's, which is also applied to the analysis of the rotational strengths.[10b] Very recently, Bouman et al.[31] carried out a localized orbital analysis on the model system such as the chiral diethyl ketone by reformulating the results of canonical calculations in terms of localized orbitals in the random phase approximation. The procedure presented in this study also lies in the course of developing the

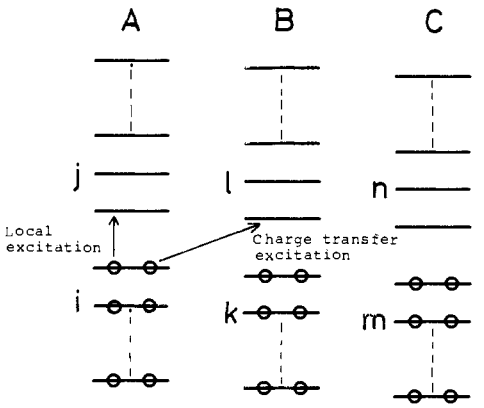

Figure 2. Schematic representation of the respective LMO's belonging to the three fragments A, B, and C in a molecule.

MO approach. Namely, we calculate the rotational strength by means of canonical MO's (CMO's) expanded into some localized MO[32] (LMO) sets belonging to the three molecular fragments, i.e., chromophore, substituent, and the rest of the molecule, by which it can be expected to evaluate simultaneously the interactions between these fragments and to extract the significant intramolecular interactions characterizing the rotational strength of interest. The standpoint of this procedure, which will be called *configuration analysis*[33,34] *based on LMO's* and will be described in the next section, is apparently close to that of the perturbation methods, since they are generally based on a model where the electrons are completely localized within the spatially separated groups in a molecule.

The purpose of the present study is to clarify the origin responsible for the rotational strengths associated with the electronic $n-\pi^*$ and $\pi-\pi^*$ transitions and also to identify the mechanism and/or path to combine the locally symmetric chromophore with the dissymmetric environment centered on the chiral position in a molecule, by evaluating the contributions of the molecular fragments to the rotational strengths. The semiempirical MO method of the MINDO/3 version[35] including configuration interaction (CI) is used for the calculations. The optically active L-5-methylpyrrolid-2-one (Figure 1) is subjected to the analysis, because it is well-known as one of the simplest molecules containing the monomeric peptide chromophore in a five-membered ring system[3,5,36,37] and hence its extensively investigated experimental[38] and theoretical[14,27] values of the rotational strengths are available for comparison with the present calculated results.

II. Theoretical Background

Expansions of CMO's and Rotational Strength by Means of LMO's. Let the n-localized SCF-MO's ϕ_d (CMO) be expressed by a linear combination of atomic orbitals (LCAO) as eq 1 and

$$\phi_d = \sum_r C_r^d \chi_r \quad r = 1, 2, ..., n \tag{1}$$

similarily n-localized MO's ϕ_f^0 (LMO) as eq 2 where the su-

$$\phi_f^0 = \sum_s C_s^{0f} \chi_s \quad s = 1, 2, ..., n \tag{2}$$

perscript 0 indicates the quantities relating to the LMO's. It should be noted that ϕ_d and ϕ_f^0 include both occupied and vacant

(15) A. Moscowitz, A. E. Hansen, L. S. Foster, and K. Rosenheck, *Biopolym. Symp.*, **1**, 75 (1964).
(16) (a) J. A. Schellman, *J. Chem. Phys.*, **44**, 55 (1966); (b) J. A. Schellman, *Acc. Chem. Res.*, **1**, 144 (1968).
(17) (a) E. G. Höhn and O. E. Weigang, Jr., *J. Chem. Phys.*, **48**, 1127 (1968); (b) O. E. Weigang, Jr., and E. G. Höhn, *J. Am. Chem. Soc.*, **88**, 3673 (1966).
(18) P. M. Bayley, E. B. Nielsen, and J. A. Schellman, *J. Phys. Chem.*, **73**, 228 (1969).
(19) W. H. Inskeep, D. W. Miles, and H. Eyring, *J. Am. Chem. Soc.*, **92**, 3866 (1970).
(20) E. C. Ong, L. C. Cusachs, and O. E. Weigang, Jr., *J. Chem. Phys.*, **67**, 3289 (1977).
(21) Y. H. Pao and D. P. Santry, *J. Am. Chem. Soc.*, **88**, 4157 (1966).
(22) R. R. Gould and R. Hoffmann, *J. Am. Chem. Soc.*, **92**, 1813 (1970).
(23) W. Hug and G. Wagniere, *Theor. Chim. Acta*, **18**, 57 (1970).
(24) A. Imamura, T. Hirano, C. Nagata, and T. Tsuruta, *Bull. Chem. Soc. Jpn.*, **45**, 396 (1972).
(25) A. Imamura, T. Hirano, C. Nagata, T. Tsuruta, and K. Kuriyama, *J. Am. Chem. Soc.*, **95**, 8621 (1973).
(26) A. P. Volosov and V. A. Zubokov, *Theor. Chim. Acta*, **44**, 375 (1977).
(27) A. P. Volosov, V. A. Zubokov, and T. M. Birshtein, *Tetrahedron*, **31**, 1259 (1975).
(28) M. B. Robin, H. Basch, N. A. Keubler, B. E. Kaplan, and J. Meinwald, *J. Chem. Phys.*, **48**, 5037 (1968).
(29) T. D. Bouman and A. E. Hansen, *J. Chem. Phys.*, **66**, 3460 (1977).
(30) D. H. Liskow and G. A. Segal, *J. Am. Chem. Soc.*, **100**, 2945 (1978).
(31) T. D. Bouman, B. Voigt, and A. E. Hansen, *J. Am. Chem. Soc.*, **101**, 550 (1979).
(32) C. Edmiston and K. Ruedenberg, *Rev. Mod. Phys.*, **35**, 457 (1963).
(33) H. Baba, S. Suzuki, and T. Takemura, *J. Chem. Phys.*, **50**, 2078 (1969).
(34) H. Fujimoto, S. Kato, S. Yamabe, and K. Fukui, *J. Chem. Phys.*, **60**, 572 (1974).
(35) R. C. Bingham, M. J. S. Dewar, and D. H. Lo, *J. Am. Chem. Soc.*, **97**, 1285, 1302 (1975).
(36) D. W. Urry, *J. Phys. Chem.*, **72**, 3035 (1968).
(37) D. F. Mayer and D. W. Urry, *Tetrahedron Lett.*, 9 (1971).
(38) (a) S. Ehenson and P. F. Phillipson, *J. Chem. Phys.*, **34**, 1224 (1961); (b) R. R. Gould and R. Hoffman, *J. Am. Chem. Soc.*, **92**, 1813 (1970).
(39) J. A. Molin-case, E. Fleischen, and D. W. Urry, *J. Am. Chem. Soc.*, **92**, 4728 (1970).
(40) J. M. Foster and S. F. Boys, *Rev. Mod. Phys.*, **32**, 300 (1960).
(41) K. Akagi, T. Yamabe, H. Kato, and K. Fukui, *J. Phys. Chem.*, **84**, 98 (1980).

orbitals. Then, the CMO's are represented by a linear combination of LMO's as

$$\phi_d = \sum_f B_f^d \phi_f^0 \tag{3}$$

where

$$B_f^d = \int \phi_d \phi_f^0 \, d\tau \tag{4}$$

In the actual case, the occupied ϕ_p^0 and vacant ϕ_q^0 LMO's are obtained from the occupied ϕ_g and vacant ϕ_e CMO's, respectively, and hence according to the Edmiston–Ruedenberg procedure,[32] eq 3 is rewritten as

$$\phi_g = \sum_p^{occ} B_p^g \phi_p^0 \tag{5-1}$$

$$\phi_e = \sum_q^{vac} B_q^e \phi_q^0 \tag{5-2}$$

Now, classifying the LMO's of a molecule into three of those fragments, A, B, and C, we can express eq 5 as

$$\phi_g = \sum_i^{occ} B_i^g \phi_i^0 + \sum_k^{occ} B_k^g \phi_k^0 + \sum_m^{occ} B_m^g \phi_m^0 \tag{6-1}$$

$$\phi_e = \sum_j^{vac} B_j^e \phi_j^0 + \sum_l^{vac} B_l^e \phi_l^0 + \sum_n^{vac} B_n^e \phi_n^0 \tag{6-2}$$

where i and j indicate the occupied and vacant LMO's of the fragment A, respectively, and similarily k and l occupied and vacant LMO's of fragment B, respectively, and so on (see Figure 2).

The reduced rotational strength $[R_{ge}]$ for the g → e transition has been given by eq 7.[21,24] With eq 6, the gradient integral of

$$[R_{ge}] = -[7313/(E_e - E_g)]\langle\phi_g|\nabla|\phi_e\rangle\langle\phi_e|\mathbf{r} \times \nabla|\phi_g\rangle \tag{7}$$

eq 7 is rewritten, i.e.

$$\begin{aligned}\langle\phi_g|\nabla|\phi_e\rangle = &\sum_i^{occ}\sum_j^{vac} B_i^g B_j^e \langle i^0|\nabla|j^0\rangle + \\ &\sum_k^{occ}\sum_l^{vac} B_k^g B_l^e \langle k^0|\nabla|l^0\rangle + \\ &\sum_m^{occ}\sum_n^{vac} B_m^g B_n^e \langle m^0|\nabla|n^0\rangle + \\ &\sum_i^{occ}\sum_l^{vac} B_i^g B_l^e \langle i^0|\nabla|l^0\rangle + \sum_i^{occ}\sum_n^{vac} B_i^g B_n^e \langle i^0|\nabla|n^0\rangle + \\ &\sum_k^{occ}\sum_j^{vac} B_k^g B_j^e \langle k^0|\nabla|j^0\rangle + \sum_k^{occ}\sum_n^{vac} B_k^g B_n^e \langle k^0|\nabla|n^0\rangle + \\ &\sum_m^{occ}\sum_j^{vac} B_m^g B_j^e \langle m^0|\nabla|j^0\rangle + \sum_m^{occ}\sum_l^{vac} B_m^g B_l^e \langle m^0|\nabla|l^0\rangle\end{aligned} \tag{8}$$

where the LMO of ϕ_i^0 is designated as i^0 and so on. The first, second, and third terms of eq 8 stand for the gradient integrals due to the intrafragmental singly excited configurations of fragments A, B, and C, respectively, and they will be named as the local excitation terms (A–A*, B–B*, and C–C*). The fourth to ninth terms stand for the gradient integrals due to the interfragmental single electron transfer configurations and will be called as the charge-transfer excitation[42] terms (A–B*, A–C*, B–A*, and so on). Similarly, the expansion formula of the magnetic moment integral is also given as the sum of the local and charge-transfer excitation terms. The reduced rotational strength is finally expressed as follows:

$$\begin{aligned}[R_{ge}] = -(7313/\Delta E_{ge})\{&(\sum_i^{occ}\sum_j^{vac} B_i^g B_j^e \langle i^0|\nabla|j^0\rangle + \dots \\ &+ \sum_m^{occ}\sum_l^{vac} B_m^g B_l^e \langle m^0|\nabla|l^0\rangle)\cdot(\sum_i^{occ}\sum_j^{vac} B_i^g B_j^e \langle j^0|\mathbf{r} \times \nabla|i^0\rangle + \dots \\ &+ \sum_m^{occ}\sum_l^{vac} B_m^g B_l^e \langle l^0|\mathbf{r} \times \nabla|m^0\rangle)\}\end{aligned} \tag{9}$$

It should be noted here that the electronic transition moments including both one and two centers are represented as dipole velocity formalism[38] and the energy difference of states ΔE_{ge} ($=E_e - E_g$) and the gradient operator ∇ are expressed in the units of eV and Å^{-1}, respectively.

Configuration Interaction. The reduced rotational strength including configuration interaction (CI) within the single excitation, $[R]_{CI}$, is given by eq 10 where ΔE_{0I} is the energy difference

$$\begin{aligned}[R]_{CI} = &(-7313/\Delta E_{0I})\langle\Psi_0|\nabla|\Psi_I\rangle\langle\Psi_I|\mathbf{r} \times \nabla|\Psi_0\rangle = \\ &(-7313/\Delta E_{0I})\{(\sum_g\sum_e C_{ge}\langle\phi_g|\nabla|\phi_e\rangle)\cdot(\sum_g\sum_e C_{ge}\langle\phi_e|\mathbf{r} \times \nabla|\phi_g\rangle)\}\end{aligned} \tag{10}$$

between the ground state and the CI excited state and C_{ge} is the CI coefficients. Applying the configuration analysis used in the previous section to the gradient integral, we rewrite the terms in the first set of parentheses of eq 10 as eq 11, where the following

$$\begin{aligned}\sum_g\sum_e C_{ge}\langle\phi_g|\nabla|\phi_e\rangle = &\sum_i^{occ}\sum_j^{vac} M_{ge}^{ij}\langle i^0|\nabla|j^0\rangle + \\ &\sum_k^{occ}\sum_l^{vac} M_{ge}^{kl}\langle k^0|\nabla|l^0\rangle + \\ &\sum_m^{occ}\sum_n^{vac} M_{ge}^{mn}\langle m^0|\nabla|n^0\rangle + \\ &\sum_i^{occ}\sum_l^{vac} M_{ge}^{il}\langle i^0|\nabla|l^0\rangle + \sum_i^{occ}\sum_n^{vac} M_{ge}^{in}\langle i^0|\nabla|n^0\rangle + \\ &\sum_k^{occ}\sum_j^{vac} M_{ge}^{kj}\langle k^0|\nabla|j^0\rangle + \sum_k^{occ}\sum_n^{vac} M_{ge}^{kn}\langle k^0|\nabla|n^0\rangle + \\ &\sum_k^{occ}\sum_j^{vac} M_{ge}^{mj}\langle m^0|\nabla|j^0\rangle + \sum_m^{occ}\sum_l^{vac} M_{ge}^{ml}\langle m^0|\nabla|l^0\rangle\end{aligned} \tag{11}$$

abreviation is used, e.g.

$$M_{ge}^{ij} = [\sum_g\sum_e C_{ge} B_i^g B_j^e] \tag{12}$$

and so on. Carrying out the same procedure with respect to the second set of parentheses of eq 12 also yields the expansion formula of the magnetic dipole integral. As a consequence, the scalar product between the gradient and magnetic dipole integrals yields the rotational strength which is expressed as the summation of the 9 × 9 coupling terms characterized by the local and charge-transfer excitations.

III. Geometries and Methods of Calculation

The geometries of planar and nonplanar ring conformations of L-5-methylpyrrolid-2-one are borrowed from the X-ray data for L-pyrrolid-2-one-5-carboxamide, in which the ring is nonplanar,[39] and are the same as those adopted by Volosov et al.[27] That is, the deviations of the pyrrolidone ring from planarity (X–Y plane) are $Z_{C_3} = -0.127$, $Z_{C_4} = 0.301$, $Z_{C_5} = 0.048$, and $Z_{H_{16}} = 0.0$ Å, respectively, and N_1, C_2, and O_6 atoms are coplanar, for the nonplanar ring conformation (see, Figure 1). It should be noted that L-5-methylpyrrolid-2-one is hereafter abbreviated as pyrrolidone, unless otherwise stated.

Calculations are carried out by the MINDO/3 scheme[29] of an SCF treatment including the configuration interaction, where the 42 singly excited states corresponding to the transition from the seven upper MO's to the six virtual MO's are considered. Although the most common procedures to obtain the LMO's have

(42) A. Denis, J. Langlet, and J. P. Malrieu, *Theor. Chem. Acta*, **29**, 117 (1973).

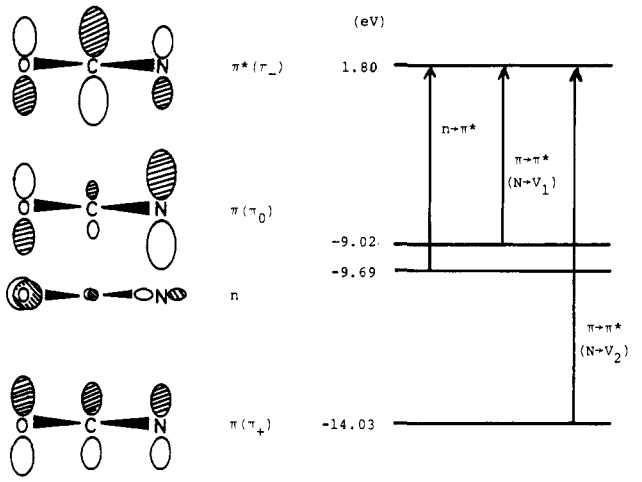

Figure 3. Some CMO's and orbital energy diagram of pyrrolidone. The values of the orbital energies are those of the nonplanar ring conformation.

Table I. Calculated Spectroscopic Properties for the n–π^* and π–π^* Transitions in L-5-Methylpyrrolid-2-one

ring conformtn	method	n–π^*		π–π^*	
		∇E^a	$[R]^b$	∇E^a	$[R]^b$
planar	INDO[c]	6.56	−11.45	10.44	2.90
	CNDO/S[d]	4.13	−4.10	7.09	3.02
	MINDO/3	4.43	−8.83	6.97	3.45
nonplanar	INDO[c]	6.97	0.44	10.41	−22.30
	CNDO/S[d]	4.13	−1.62	7.09	16.63
	MINDO/3	4.49	−2.88	6.99	4.84
exptl[e]		5.77	−7.34	6.70	13.50

[a] Energies in eV. [b] $[R] = 1.08 \times 10^{40}$ R (cgs). [c] Reference 14. [d] Reference 27. [e] Reference 36.

been the Edmiston–Ruedenberg[32] and the Foster–Boys[40] methods, the latter tends to yield "banana" bonds instead of the more conventional σ–π orbitals for the mutiple bond. Therefore, we employed the former in the present LMO calculations.

IV. Results and Discussion

(A) Direct MO Calculations. In Figure 3 are shown some important CMO's and the orbital energy diagram of pyrrolidone. The orbital interaction between the nitrogen lone-pair orbital being perpendicular to the X–Y plane (π_N) and the carbonyl π orbital ($\pi_{C=O}$) yields the two kinds of π orbitals, π_0 and π^+, and the corresponding antibonding π orbital, π_-.[43] Among the electronic transitions between these orbitals, we will consider the $\pi_0 \rightarrow \pi_-$ ($N \rightarrow V_1$) transition as well as the $n_0 \rightarrow \pi_-$ one, and hereafter abbreviate them as π–π^* and n–π^* transitions, respectively, for simplicity. Table I summarizes the rotational strengths, $[R]$, and the energy difference of the states corresponding to the excitation energies, ΔE for the n–π^* and π–π^* and π–π^* transitions of pyrrolidone calculated by the MINDO/3-CI method, together with other calculated and experimental values. It is found from this table that the calculated results by the present method as well as those by the CNDO/S method are more favorable than those by the INDO method in comparison with the experimental values. Especially, the agreements between the experimental and our calculated excitation energies for both n–π^* and π–π^* transitions are better than those in the other cases. It is desired at this stage to decide which ring conformation of pyrrolidine is more acceptable from the analysis of the rotational strengths, since the structure of such a methyl-substituted pyrrolidone has not yet been studied experimentally. The comparison of relative magnitudes between the experimental and calculated kinds of rotational strengths would lead to the choice of the nonplanar ring conformation. That is, the relative magnitude between the calculated n–π^* (−2.88) and π–π^* (4.84) rotational strengths in the nonplanar ring conformation is in excellent agreement with the case of the experimental values, where the n–π^* rotational strength (−7.34) is almost half of the π–π^* one (13.50), although only the n–π^* rotational strength (−8.83) in the planar ring conformation is fairly close to the corresponding value. The preference of the nonplanar ring conformation thus argumented is consistent with that of Volosov et al.[27] and also supported by the experimental X-ray data of pyrrolidone derivatives, the ring of which is nonplanar.[39] Therefore, we will hereafter employ the nonplanar ring conformation of pyrrolidone for the analysis of the rotational strengths.

Now, it is worthwhile to examine the effect of CI and the contributions of the cartesian components of the rotational strengths. Table II shows the components of the gradients and magnetic dipole integrals and also their scalar products on the rotational strengths before and after CI calculations. It is seen that the rotational strengths after CI are well improved in the sign and magnitude compared with those before CI, the values of which are overestimated throughout. At the same time, the remarkable changes in the contributions of the Cartesian components of the rotational strengths are found; in the n–π^* rotational strength, the Z components of the scalar product, $[\nabla\cdot(r \times \nabla)]_Z$, become more contributive than other components after CI, in spite of the dominant contributions of the Y component before CI. A similar trend is found in the case of the π–π^* rotational strength. Especially, it should be emphasized that the CI procedure is indispensable in getting the correct sign for the π–π^* rotational strength, since the value before CI is opposite in sign to the corresponding experimental value.

(B) Expansion of CMO's in Terms of LMO's. The LMO expansion coefficients and their weights for the CMO's of interest are obtained according to eq 5 presented in section II. By classifying the LMO's of pyrrolidone into three molecular fragments, i.e., carbonyl chromophore, parent molecule, and methyl substituent, which are being designated as A, B, and C fragments, respectively (Figure 1), one can represent the CMO's in terms of the LMO's belonging to each molecular fragment. The results thus obtained are shown in Table III. It is straightforward from this table to evaluate quantitatively the degree of the localization and/or delocalization of the CMO's. The canonical lone-pair orbital (n-CMO), which should be assigned to the carbonyl-oxygen lone-pair orbital (n_O), is largely delocalized over the parent molecule. The antibonding π orbital (π^*–CMO), which is mainly characterized by the $\pi^*_{C=O}$ orbital, also shows a trend of delocalization, centered around the carbon (C_3) atom adjacent to the carbonyl group of pyrrolidone. Such a feature of the delocalization of the n and π^* CMO's indicates that n–π^* transition of pyrrolidone has a nature of electronically dipole allowedness to a certain extent.[41] This nature is generated by the molecular distortion such as the deviation of the ring from the planarity associated with the substitution of the heteroatom (nitrogen) or methyl group into the five-membered ring. Meanwhile, the π-CMO, which has inherently the natures of both the nitrogen lone-pair orbital being perpendicular to the X–Y plane (π_N) and the carbonyl π orbital ($\pi_{C=O}$) as shown in Figure 3, is found to be considerably delocalized around the asymmetric carbon (C_5) atom linked with the methyl substituent. It is therefore expected that the rotational strength due to the π–π^* transition is more sensitively affected by the dissymmetric environment centered on the methyl fragment of pyrrolidone than the case of the n–π^* rotational strength.

Table IV shows the weights of configurations of the local and charge-transfer excitations after CI calcultions (e.g., the weight of the configuration for the local excitation on the A fragment is given as $\sum_i^{occ}\sum_j^{vac}(\sum_g\sum_e C_{ge}B_i^g B_j^e)^2$). The configurations of the local excitation on the carbonyl chromophore, A–A*, and the charge-transfer excitation from the parent molecule to the carbonyl chromophore, B–A*, are found to have a significant role in characterizing the optical properties associated with the n–π^* transition, and the A–B* and B–B* type configurations are of secondary importance. As for the case of the π–π^* transition,

(43) (a) H. D. Hunt and W. T. Simpson, *J. Am. Chem. Soc.*, **75**, 4540 (1953); (b) D. L. Peterson and W. T. Simpson, *ibid.*, **79**, 2375 (1967); (c) H. Basch, M. B. Robin, and N. A. Kuebler, *J. Chem. Phys.*, **47**, 1201 (1967); (d) M. A. Robb and I. G. Csizmadia, *ibid.*, **50**, 1819 (1969).

Table II. Components of the Gradient and Magnetic Dipole Integrals for the n–π^* and π–π^* Transitions in the Nonplanar Pyrrolidone

			X	*Y*	*Z*	total
n–π^*	before CI	$\nabla_i \times 10^2$	−6.306	−1.694	6.234	
		$(r \times \nabla)_i \times 10^2$	2.216	−52.07	1.851	
		$[\nabla\cdot(r \times \nabla)]_i \times 10^3$	−1.397	8.819	1.154	8.575
	after CI	$\nabla_i \times 10^2$	1.763	−0.085	−3.579	
		$(r \times \nabla)_i \times 10^2$	4.007	56.18	−4.091	
		$[\nabla\cdot(r \times \nabla)]_i \times 10^3$	0.706	−0.474	1.538	1.770
π–π^*	before CI	$\nabla_i \times 10^2$	−22.22	27.45	−3.027	
		$(r \times \nabla)_i \times 10^2$	3.216	10.32	−4.917	
		$[\nabla\cdot(r \times \nabla)]_i \times 10^3$	−7.145	28.34	1.480	22.770
	after CI	$\nabla_i \times 10^2$	0.878	−3.126	2.278	
		$(r \times \nabla)_i \times 10^2$	10.26	2.409	−20.95	
		$[\nabla\cdot(r \times \nabla)]_i \times 10^3$	0.900	−0.753	−4.772	−4.625

Table III. Expansion Coefficients and Weights of LMO's in n-, π-, and π^*-CMO's in Terms of Three Fragments, Carbonyl Group (A), Parent Molecule (B), and Methyl Substituent (C)

		n-CMO		π-CMO		π^*-CMO	
fragment	LMO's	expans coeff	% wt	expans coeff	% wt	expans coeff	% wt
A	n_O	0.489	23.91	−0.066	0.44		
	n_O	−0.478	22.85	−0.158	2.50		
	C=O(π)	0.024	0.06	−0.286	8.18	−0.823	67.73
	C=O(σ)	0.011	0.01	−0.037	0.14	0.056	0.31
			(46.83)		(11.26)		(68.04)
B (path 1)	C_2–N_1	−0.365	13.32	−0.282	7.95	0.116	1.35
	n_N	0.057	0.32	−0.572	32.72		
	N–N	0.091	0.83	−0.174	3.03	−0.076	0.58
	C_5–N_1	0.254	6.45	−0.114	1.30	−0.041	0.17
			(20.92)		(45.00)		(2.10)
B (path 2)	C_4–C_5	−0.154	2.37	−0.001	0.00	−0.065	0.42
	C_3C_4	−0.125	1.56	−0.012	0.01	−0.045	0.20
	C_1–C_3	−0.410	16.81	−0.011	0.01	0.105	1.10
	C_4–H_{10}	0.041	0.17	0.081	0.66	0.038	0.14
	C_4–H_{11}	0.185	3.42	−0.089	0.79	0.095	0.90
	C_3–H_8	−0.060	0.36	−0.041	0.17	0.244	5.95
	C_3–H_9	−0.122	1.49	0.043	0.18	0.372	13.83
			(22.18)		(1.82)		(22.54)
C	C_5–C_7	−0.001	0.00	0.432	18.66	0.112	1.25
	C_5–H_{15}	−0.119	1.42	0.430	18.49	0.221	4.88
	C_7–H_{12}	0.048	0.23	−0.212	4.41	−0.027	0.07
	C_7–H_{13}	0.128	1.63	0.046	0.21	−0.003	0.01
	C_7–H_{14}	0.166	2.76	−0.021	0.04	−0.102	1.04
			(6.04)		(41.81)		(7.25)
			99.97		99.89		99.93

the fairly large weights of the charge-transfer excitation from the methyl substituent to the carbonyl chromophore, C–A*, and to the parent molecule, C–B*, are worthy to note. This partly reflects the delocalized character of the π-CMO as mentioned above.

(C) Analysis of the Rotational Strengths. Now we are able to partition the rotational strengths obtained with CI calculations into the contributions from the intra- and interfragmental electronic configurations on the basis of three fragments of the pyrrolidone molecule. The results of analyses for the n–π^* and π–π^* rotational strengths are shown in Tables V and VI, respectively. The values of matrices in these tables are given as the scalar products of the vectors of each molecular fragment corresponding to the gradient and magnetic dipole operators, without multiplying by the constant (−7313) and also without dividing by the excitation energies (ΔE = 4.49 and 6.99 eV for the n–π^* and π–π^* transitions, respectively), as represented in Table II. Hence it should be noted that the total values of the scalar products in these tables are opposite in sign to those of the reduced rotational strengths (see also Tables I and II). It can be seen from Tables V or VI that among the 9 × 9 coupling terms produced between the gradient and magnetic dipole integrals, the total value of the scalar product is decided by some positive and negative coupling terms. These couplings are futhermore schematically illustrated in Figures 4 and 5, together with the corresponding values, in order to illuminate the essential feature of the interaction between these fragments.

Concerning the n–π^* rotational strength (Table V and Figure 4), the five positive couplings are recognized to dominantly contribute with the same sign to the total scalar product in the following order: ∇(B–B*)·r × ∇(A–A*) ≃ ∇(C–C*)·r × ∇(B–A*) > ∇(B–B*)·r × ∇(C–B*) ≃ ∇(B–A*)·r × ∇(C–C*) ≃ ∇(B–A*)·r × ∇(B–B*). The negative couplings also being important ones, on the other hand, are as follows: ∇(B–B*)·r × ∇(B–A*) ≃ ∇(B–B*)·r × ∇(B–B*) ≃ ∇(B–A*)·r × ∇(A–A*) > ∇(B–A*)·r × ∇(B–A*). It is evident that the local excitation on the carbonyl chromophore or the parent molecule and the

Table IV. Weights (%) of the Electronic Configurations for the Local and Charge-Transfer Excitations after CI Calculation

		n–π^*		π–π^*	
A–A*			37.36		1.08
B–B*	path 1–path 1*	1.19		0.65	
	path 2–path 2*	6.40	12.46	6.78	31.15
	path 1–path 2*	4.71		23.17	
	path 2–path 1*	0.16		0.55	
C–C*			0.16		6.65
A–B*	A-path 1*	0.64	13.98	0.78	14.97
	A-path 2*	13.32		14.10	
B–A*	path 1–A*	13.28	30.85	5.10	6.89
	path 2–A*	17.57		1.79	
A–C*			1.70		1.98
C–A*			0.80		11.86
B–C*	path 1–C*	0.82	1.55	1.75	3.75
	path 2–C*	0.73		2.00	
C–B*	C-path 1*	0.72	0.88	0.68	21.36
	C-path 2*	0.16		20.68	
total			100.00		99.72

Table V. Partition of the n-π^* Rotational Strength into (9 × 9) Electronic Configurations Based on the Three Molecular Fragments (Values × 10^4)

	r × ∇									
∇	A-A*	B-B*	C-C*	A-B*	B-A*	A-C*	C-A*	B-C*	C-B*	total
A-A*	2.35	−3.58	−5.79	2.43	0.02	−0.44	0.53	−2.95	−0.29	−7.74
B-B*	32.03	−21.29	2.95	−0.30	−21.88	−0.22	−1.60	2.35	14.56	6.60
C-C*	3.49	4.23	−0.53	1.02	31.21	0.26	0.45	0.72	−1.05	39.79
A-B*	−4.71	2.97	−0.37	−0.00	2.30	0.03	0.21	−0.34	−2.06	−1.97
B-A*	−20.71	13.08	13.39	−6.66	−18.55	0.93	−1.06	5.66	−3.86	−17.79
A-C	1.26	0.01	−0.30	0.26	4.07	0.01	0.06	0.01	0.13	5.50
C-A*	0.24	−0.59	−0.53	0.20	1.20	−0.05	0.03	−0.30	0.07	−2.14
B-C*	2.05	0.26	−1.81	1.03	10.35	−0.04	0.29	−0.58	−0.34	11.21
C-B*	2.40	−0.98	0.05	−0.36	−11.43	−0.10	−0.12	−0.39	−0.08	−15.80
total	13.59	−5.90	7.06	−2.38	−5.11	0.38	−1.21	4.17	7.07	17.67

Table VI. Partition of the π-π^* Rotational Strength into (9 × 9) Electronic Configurations Based on the Three Molecular Fragments (Values × 10^4)

	r × ∇									
∇	A-A*	B-B*	C-C*	A-B*	B-A*	A-C*	C-A*	B-C*	C-B*	total
A-A*	1.33	−56.53	−41.28	−1.30	−0.27	−0.54	−16.14	9.00	5.13	−100.60
B-B*	−25.87	2.85	1.96	−5.63	−12.95	−0.23	3.64	22.00	−4.69	−18.85
C-C*	−18.32	19.03	6.72	−1.47	−7.89	0.26	5.73	9.68	6.60	20.34
A-B*	0.32	3.54	13.39	−2.94	−1.31	−0.34	3.49	3.51	−17.64	2.01
B-A*	50.97	46.33	33.01	12.89	26.53	0.99	7.28	−53.28	6.51	131.23
A-C*	−0.77	−1.28	−0.30	−0.39	−0.50	−0.04	−0.13	1.16	−1.05	−3.30
C-A*	−2.70	4.35	−3.73	1.51	0.31	0.26	−0.08	−1.25	10.25	8.23
B-C*	5.06	−27.51	−9.03	−2.84	0.52	−0.61	−5.76	5.04	−14.51	−49.62
C-B*	−4.39	−16.81	−5.90	−3.14	−3.31	−0.41	−0.41	9.18	−8.92	−35.79
total	5.63	−25.40	−5.16	−3.31	0.52	−0.66	−4.68	5.10	−18.32	−46.28

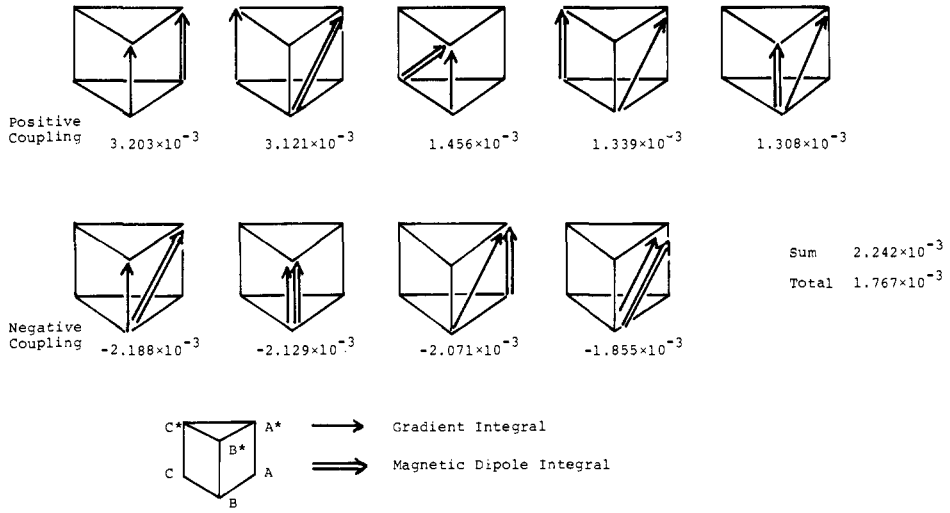

Figure 4. Coupling diagram for the n-π^* transition: schematic representation for some electronic configurations making a large contribution to the product of the gradient and magnetic dipole integrals.

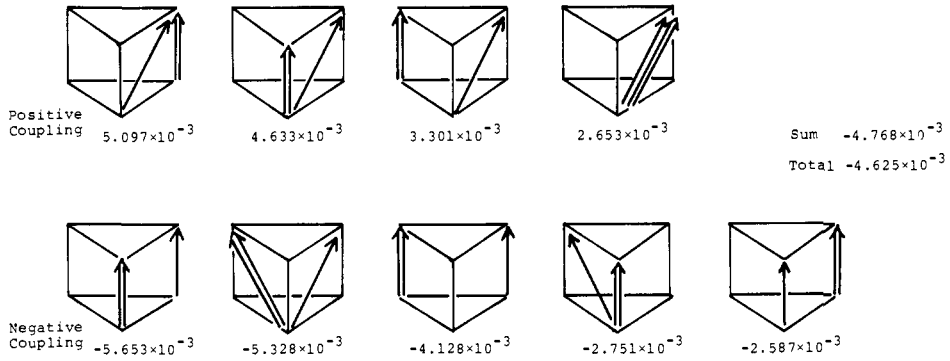

Figure 5. Coupling diagram for π-π^* transition.

charge-transfer excitation from the parent molecule to the carbonyl chromophore have a significant role in common with the positive and negative couplings between the gradient and magnetic dipole integrals. Hence, it follows that the intramolecular interaction between the carbonyl chromophore and the parent molecule through the above-mentioned electronic configurations is primarily

Table VII. Contributions of the Local and Charge-Transfer Excitation Terms in the Gradient and Magnetic Dipole Integrals (Z Component) for the n–π^* Transition (Values $\times 10^2$)

	∇_Z for π^* =				$(r \times \nabla)_Z$ for π^* =			
n	C=O	path 1	path 2	CH_3	C=O	path 1	path 2	CH_3
C=O	2.793	0.219	0.062	0.112	−0.024	0.424	0.380	−0.283
path 1	13.233	2.441	−0.192	1.246	−0.212	0.063	0.908	−0.419
path 2	−19.309	0.037	−4.288	−0.424	−0.309	1.013	−2.745	−0.668
CH_3	0.258	0.154	−0.102	0.121	0.202	0.032	−0.422	−2.031
total		−3.579				−4.091		

Table VIII. Contributions of the Local and Charge-Transfer Excitation Terms in the Gradient and Magnetic Dipole Integrals (Z Component) for the π–π^* Transition (Values $\times 10^2$)

	∇_Z for π^* =				$(r \times \nabla)_Z$ for π^* =			
π	C=O	path 1	path 2	CH_3	C=O	path 1	path 2	CH_3
C=O	5.502	0.064	−0.456	0.092	−0.049	0.928	−1.553	−0.148
path 1	−0.832	0.745	−0.347	−0.322	0.399	−2.516	0.824	1.990
path 2	−2.109	−0.032	−1.214	2.794	−0.758	−1.370	−8.300	0.513
CH_3	−0.394	0.310	0.981	−2.054	−2.970	2.580	−3.250	−7.274
total		2.278				−20.950		

contributive to the n–π^* rotational strength we are concerned with here. At the same time, the relatively large absolute values of the positive and negative couplings with respect to this intramolecular interaction may imply that the n–π^* rotational strength, especially its sign, is sensitive to the ring chirality attributed to the molecular distortion with the lowering of the symmetry and to the deviation of the pyrrolidone ring from planarity. These arguments are consistent with those of other extensive studies.[12a,c,27] It should be noted furthermore that the local excitation on the methyl substituent coupled with the charge-transfer excitation from the parent molecule to the carbonyl chromophore, ∇(C–C*)·r × ∇(B–A*) or ∇(B–A*)·r × ∇(C–C*), plays an important role in the intensification of the n–π^* rotational strength; the signs of these couplings are the same (positve) as that of the total scalar product. This means that the chirality of the asymmetric methyl substituent does not directly affect the locally symmetric carbonyl chromophore but indirectly affects it through the charge-transfer excitation from the parent molecule to the carbonyl chromophore.

On the other hand, one can select the following important couplings on the π–π^* rotational strength (Table VI and Figure 5): ∇(B–A*)·r × ∇(A–A*) > ∇(B–A*)·r × ∇(B–B*) > ∇(B–A*)·r × ∇(C–C*) > ∇(B–A*)·r × ∇(B–A*) for the positive couplings and ∇(A–A*)·r × ∇(B–B*) ≃ ∇(B–A*)·r × ∇(B–C*) > ∇(A–A*)·r × ∇(C–C*) > ∇(B–B*)·r × ∇(A–A*) > ∇(C–C*)·r × ∇(A–A*) for the negative couplings. Both the local excitation on the carbonyl chromophore or the parent molecule and the charge-transfer excitation from the parent molecule to the carbonyl chromophore are confirmed to be signficant, which suggests a considerable importance of the intramolecular interaction between the carbonyl chromophore and the parent molecule on the π–π^* rotational strength, as is the case in the n–π^* rotational strength. In addition, it is desired to emphasize certain negative couplings concerning the methyl substituent in order to explain the resultant negative value of the total scalar product. That is, one of them is the coupling of ∇(B–A*)·r × ∇(B–C*), which makes it possible to combine the carbonyl chromophore with the methyl substituent through the parent molecule by means of the charge-transfer excitation. Another is ∇(A–A*)·r × ∇(C–C*) or ∇(C–C*)·r × ∇(A–A*), which indicates the indirect interaction between the carbonyl chromophore and methyl substituent through the polarization mechanism associated with the local excitations on spatially separated molecular fragments. As a consequence, the intramolecular interaction between the carbonyl chromophore and methyl substituent through the above-mentioned mechanisms makes an indispensable contribution to the determination of the sign and magnitude for the π–π^* rotational strength, as well as that between the carbonyl chromophore and the parent molecule as discussed above.

(D) Indentification of the Path Generating the Rotational Strength. Next, let use consider the second subject, the identification of the path generating the rotational strength from the aspect of the through bond interaction. To do this, it is convenient to divide further the parent molecule (B fragment) into the two parts of the ring skeleton, the short and long zigzag skeletons being designated as paths 1 and 2, respectively, shown in Figure 1. Such a division with respect to the B fragment can be easily achieved with a similar procedure previously mentioned (see, Tables III and IV). It follows therefore that the results presented in this section are based on the more detailed analysis of the rotational strengths than those of the previous section. Before partitioning of the rotational strength in terms of the A, path 1, path 2, and C fragments, it may be desired to remember that the Cartesian Z components of the scalar products between the gradient and magnetic dipole intergrals for both n–π^* and π–π^* rotational strengths calculated with CI are more and/or predominantly contributive than the other components (see Table II). Hence, it can be admitted for the brevity of the discussion to consider only the Z components of the gradient and magnetic dipole integrals and their scalar product. The results obtained for the n–π^* and π–π^* rotational strengths are shown in Tables VII and VIII, respectively.

Table VII indicates that the charge-transfer excitations from both path 1 and path 2 to the carbonyl chromophore in the gradient integral make the predominant contributions, and the difference between the values of corresponding terms, in which the latter is larger than the former, primarily determines the total value of the gradient integral. This means that when the n–π^* electronic transition is regarded as the local transition on the locally symmetric carbonyl chromophore, it is more strongly affected by the dissymmetric environment through the long-range zigzag skeleton, path 2, than through the short-range zigzag skeleton, path 1. At the same time, it is clear from this analysis that the charge-transfer excitation with respect to paths 1 and 2 are particularly important in combining directly the carbonyl chromophore with the parent molecule, and the corresponding dominant values with the signs being opposite to each other strongly confirm the sensitivity of the n–π^* rotational strength to the ring chirality discussed in the previous section. Furthermore, these two significant charge-transfer excitations in the gradient integral are verified to couple effectively with the local excitations on path 2 and methyl substituent in the magnetic dipole integral, which results in the dominant couplings determining the total scalar product for the n–π^* rotational strength, as shown in Figure 6. From these results, the following conclusive argument can be drawn: the long-range zigzag path is the most important path generating the n–π^* rotational strength, which is coincident with the experimental fact that the structural change of the pyrrolidone ring mainly with respect to the long-range zigzag skeleton produces the opposite CD sign of this transition.[12d] The above concluding remark is also consistent with the result of the chiral conformation

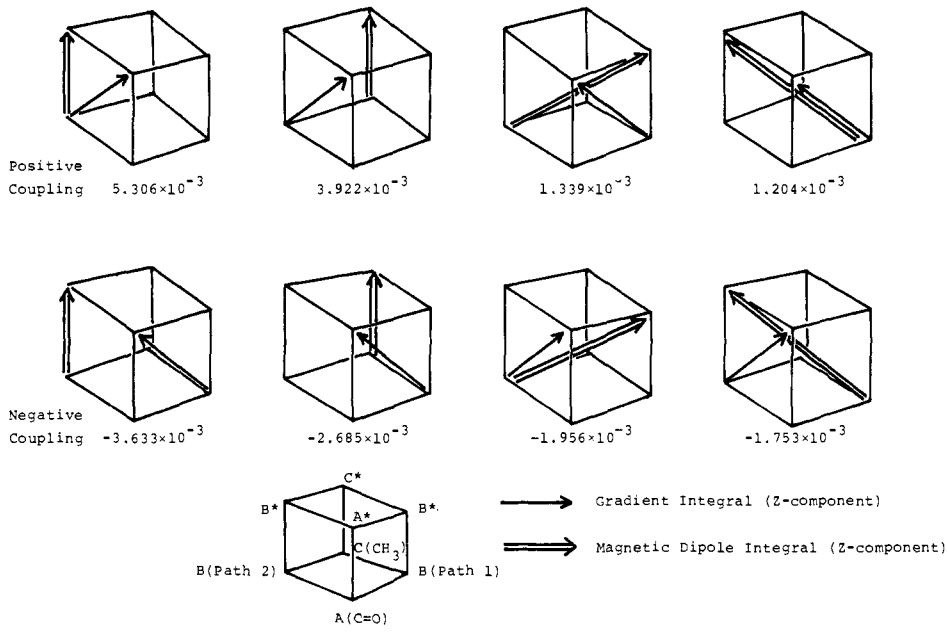

Figure 6. Coupling diagram for n–π^* transition.

of diethyl ketone given by Bouman et al.[31] that the contribution from the long-range coupling (charge transfer between the zigzag bonds and the carbonyl group) is much more significant for the induced electronic n–π^* transition moment.

Meanwhile, it is recognized from Table VIII that the local excitation on the carbonyl chromophore plays a central role in the intensification of the gradient integral corresponding to the dipole strength for the π–π^* transition, in spite of the small weight of the A–A* type electronic configuration (Table IV). This is mainly due to the large absolute value of the gradient integral of the electronically allowed $\pi_{C=O}$–$\pi^*_{C=O}$ transition, $\langle\pi_{C=O}|\nabla|\pi^*_{C=O}\rangle$. Then, it may be preferable to examine the electronic configurations in the magnetic dipole integral for the identification of the essential path and/or mechanism in question. The local excitations on path 2 and methyl substituent make the primary contributions in the magnetic dipole integral, the trend of which also has been found in the case of the n–π^* rotational strength. Besides, the charge-transfer excitation from the methyl substituent to path 2 is of secondary importance. Therefore, it can be reasonable to say that in the π–π^* rotational strength the long-range zigzag path linked with the skeleton of the asymmetric methyl substituent is a major path in bringing about the dissymmetric nature in the locally symmetric carbonyl chromophore.

Lastly, we are tempted to comment on the the source generating the difference between paths 1 and 2 in the contributions to the rotational strength of pyrrolidone. That is, the greater importance of path 2 over path 1 in common with the n–π^* and π–π^* rotational strengths thus obtained may be rationalized by reexamining the feature of the delocalization of the π^*-CMO. As found in Table III, the weights of the expansion in the π^*-CMO in terms of the vacant C_3–H_8 (equatorial C_α–H) and C_3–H_9 (axial C_α–H) LMO's are relatively large values, which are ascribed to the fact that the π^*-CMO tends to be delocalized around the C_3 (C_α) atom on the long-range zigzag skeleton (path 2) as well as the carbonyl group, $H_2C_\alpha C{=}O$ fragment. The results that the electronic

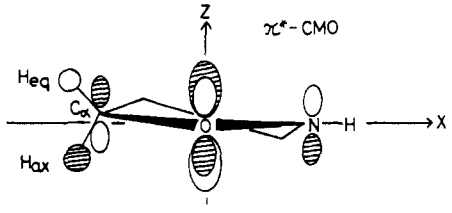

configurations with respect to path 2 are throughout larger than those concerning path 1 in both n–π^* and π–π^* transitions after CI (Table IV) reflect such a condition for the delocalization of the π^*-CMO. In other words, it follows therefore that C_α–H bonds, especially the axial C_α–H one, make an indispensable role in characterizing both n–π^* and π–π^* rotational strengths of pyrrolidone, the argument of which seems to be consistent with those of the n–π^* rotational strengths of the chiral cyclopentanone ring systems.[44]

V. Conclusion

The analysis of the rotational strengths on the optically active pyrrolidone molecule has been achieved from the point of view of origin, path, and mechanism generating the rotational strengths, for which the contributions of the three or four molecular fragments of a molecule to the rotational strength have been evaluated by using configuration analysis based on LMO's proposed here. From the present study, the following concluding remarks will be drawn:

(1) The n–π^* rotational strength of pyrrolidone is preferably determined by the intramolecular interaction between the carbonyl chromophore and the parent molecule through both the charge-transfer excitation from the parent molecule to the carbonyl chromophore and local excitations on these fragments, which may lead to the primary importance of the inherent ring chirality as the origin responsible for this rotational strength. The effect of the asymmetric substituted methyl group, which comes from the electronic–magnetic dipole coupling between the local excitation on the methyl substituent and the charge-transfer excitation from the parent molecule to the carbonyl chromophore, also plays a significant role in the intensification of this rotational strength.

The long- and short-range zigzag skeletons defined on the pyrrolidone ring are identified to be predominant paths affording the reverse contributions to each other for the n–π^* rotational strength as well as the corresponding dipole strength, which may be correlated with the sensitivity of the rotational strength to the ring structure. The methyl substituent which extends the long-range zigzag path gives a same-signed contribution of rotational strength with the aid of the polarization mechanism, that is, local excitation.

(2) In the π–π^* rotational strength, the indirect interaction between the carbonyl chromophore and the methyl substituent through the parent molecule, arising from the mechanism of the charge-transfer excitations, and the indirect interaction between them through the polarization mechanism associated with the local excitations are found to be indispenable, as well as the intramo-

(44) D. N. Kirk, *J. Chem. Soc., Perkin Trans. 1*, 2171 (1976); see also D. N. Kirk and W. Klyne, *ibid.*, 762 (1976).

lecular interaction between the carbonyl chromophore and the parent molecule. It is therefore more suitable to express that the origin of this rotational strength is the inherent ring chirality combined with the asymmetrically substituted methyl group.

The long-range zigzag path linked with the skeleton of the methyl substituent is identified to be a major path, making the locally symmetric carbonyl chromophore effectively couple with the dissymmetric environment, which is also consistent with the above-mentioned argument concerning the origin of this rotational strength.

Lastly, we are tempted to comment on the advantage of the present procedure and its possible extension. The expansion of CMO's in terms of LMO's makes it possible to evaluate quantitatively the degree of the localization and/or delocalization of CMO's concerned. The division of LMO's into the belonging fragment in this expansion enables one to make a discussion from the aspect of group MO's, which is useful for the characterizations of several kinds of substituents and chromophores. The electronic structural terminologies such as local and charge-transfer excitations derived from this procedure are helpful in understanding the intramolecular interactions. The approach using this procedure is promising for elucidating not only the essential feature of the coupling between the electronic and magnetic dipole transitions but also the origin and effective path generating the rotational strength, which neither the perturbation method nor the usual MO calculation can rationalize with sufficient accuracy. The application of the present procedure with some modifications to the induced CD, magnetic rotational strength, and other physical properties on the three or four interacting systems also will be available in the near future.

Acknowledgments. This work was supported by a Grant-in-Aid for Scientific Research from the Ministry of Education of Japan, for which we express our gratitude. The computations were carried out on a FACOM M190 at the Data Processing Center, Kyoto University.

Metastable Decompositions of $C_5H_{10}O^{+\cdot}$ Ions with the Oxygen on the Middle Carbon: A Test for Energy Randomization

David J. McAdoo,* William Farr, and Charles E. Hudson

Contribution from the Marine Biomedical Institute and Department of Human Biological Chemistry and Genetics, University of Texas Medical Branch, Galveston, Texas 77550.
Received February 11, 1980

Abstract: This study was undertaken to define the mechanisms of metastable decomposition of $C_5H_{10}O^{+\cdot}$ ions with the oxygen on the middle carbon, and to test the assumption that internal energy becomes randomly distributed prior to the unimolecular decompositions of gaseous ions. $CH_3CH_2C(=OH^+)CH_2CH_2\cdot$ (**2**), $CH_3CH_2C(=OH^+)\cdot CHCH_3$ (**3**), and $CH_3CH_2C(OH^+\cdot)HCH=CH_2$ (**4**) all rearrange to $CH_3CH_2C(=O^+\cdot)CH_2CH_3$ (**1**) prior to metastable decomposition. However, **2**–**4** lose ethyl 50–100 times as often as they lose ethane following rearrangement to **1**, while **1** formed by ionization of 3-pentanone loses exclusively ethane. These differences are attributed to excess energy in the isomerized ions. 3-Pentanone ions formed by isomerization of **2**–**4** lose ethyl and ethane from opposite sides at unequal rates, possibly owing to incomplete randomization of energy following isomerization.

The quasi-equilibrium theory of mass spectrometry (QET) is based on the assumption that energy becomes randomly distributed among all internal degrees of freedom of a reactant ion more rapidly than reaction occurs.[1] If this assumption is valid, the decomposition pattern of an ion with a given internal energy will not depend on its mode of preparation.[2,3] Metastable decompositions are thought to be competitive processes, generally taking place over a narrow range of energies just above the threshold for decomposition. However, metastable decomposition patterns can vary with the energy content of the decomposing ion,[4] which in turn can be a function of the mode of preparation.[5,6] The energy randomization assumption of the QET can be tested by comparing the decompositions of metastable ions of the same structure prepared in different ways to see whether the patterns depend on the mode of ion preparation.[2,7] In support of the QET assumption, the decomposition patterns of many metastable ions with the same structure but different origins are very similar.[2,3] These tests are valuable, since they do not involve vibrational frequencies for ions and activated complexes, which are not available and must be estimated to carry out QET calculations. One such test is whether symmetric ions chemically activated by isomerization on one side lose symmetrically placed groups at equal rates.[8,9] The enolic isomer of the acetone ion apparently violates the energy randomization assumption of the QET upon metastable decomposition.[8] This rearranges to the symmetric acetone ion and then loses CH_2H^0 about 1.3 times as often as it loses CH^a_3 (Scheme I). The inequality in the reaction rates was attributed to concentration of internal energy on the side of the ion on which rearrangement occurs, with decomposition taking place faster than

Scheme I

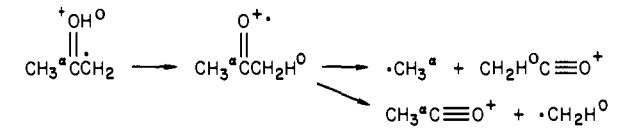

Scheme II

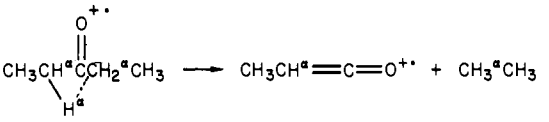

(1) Rosenstock, H. M.; Wallenstein, M. B.; Wahrhaftig, A. L.; Eyring, H. *Proc. Natl. Acad. Sci. U.S.A.* **1952**, 38, 667–678.
(2) Rosenstock, H. M.; Dibeler, V. H.; Harllee, F. N. *J. Chem. Phys.* **1964**, *40*, 591–594.
(3) Shannon, T. W.; McLafferty, F. W. *J. Am. Chem. Soc.* **1966**, *88*, 5021–5022.
(4) Yeo, A. N. H.; Williams, D. H. *J. Am. Chem. Soc.* **1971**, *93*, 395–400.
(5) Hvistendahl, G.; Williams, D. H. *J. Am. Chem. Soc.* **1975**, *97*, 3097–3101.
(6) Williams, D. H. *Acc. Chem. Res.* **1977**, *10*, 280–286.
(7) Rosenstock, H. M. *Adv. Mass Spectrom.* **1968**, *4*, 523–545.
(8) McLafferty, F. W.; McAdoo, D. J.; Smith, J. S.; Kornfeld, R. *J. Am. Chem. Soc.* **1971**, *93*, 3720–3730.
(9) Griffin, L. L.; McAdoo, D. J. *J. Phys. Chem.* **1979**, *83*, 1142–1144.

0002-7863/80/1502-5165$01.00/0